CHAPTER 12.22

Manganese

William M. Cross and Jon J. Kellar

Manganese, Mn, element 25 in the periodic table, is the 12th most abundant element in the earth's crust, with ~1,000 ppm (~0.1%) concentration and the fourth most-used metal after iron, aluminum, and copper (Gulf Manganese Corporation 2015). As can be seen in Figure 1, manganese metal is not stable in water and therefore is not found in nature in its metallic state. The primary stable manganese oxide/hydroxide minerals are also shown in the figure. The use of manganese minerals by humans dates back at least 22,000 years before present in the "Entrance Gallery" of the Gargas cave in the Hautes-Pyrénées, France. These Paleolithic people mixed manganite (γ-MnOOH) and cryptomelane ((K,Ba) (Mn^{2+}, Mn^{4+})$_8O_{16}\cdot xH_2O$) with pyrolusite (MnO_2), calcite, and clay binders, and with hollandite (Ba(Mn^{2+}, Mn^{4+})$_8O_{16}$) without binders, to produce slightly different dark colors to adjacent hand prints (Chalmin et al. 2006). This use seems deliberate because, for instance, manganite and hollandite do not generally occur together because of their different thermogeochemical origins.

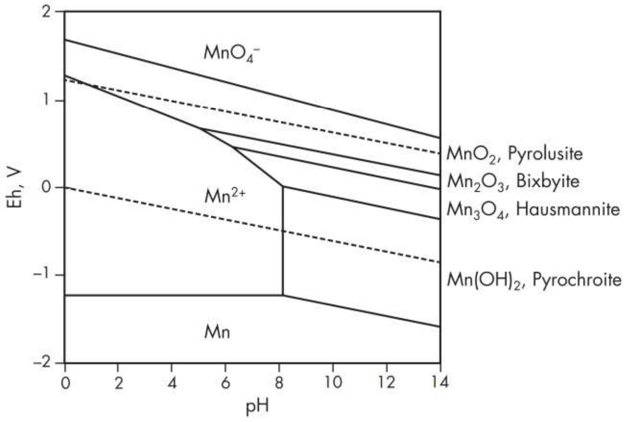

Note: Diagram was generated using Stabcal software (Huang 2012) with the Minteq (Gustafsson 2015) database and assuming a manganese concentration of 2,000 ppm. The dashed lines represent the water stability region.

Figure 1 Pourbaix diagram for the Mn–H_2O system

METAL/MINERAL USAGE

Manganese has several uses. The largest use is in the steel industry, which typically consumes about 90% of the manganese produced each year (Gulf Manganese Corporation 2015a). Other important uses include batteries and electronics, aluminum and copper alloys, fertilizers and micronutrients, water treatment, and as a colorant in materials, including glass, textiles, and plastic (Matos and Corathers 2005).

Steel production typically uses 6–9 kg Mn per metric ton of steel produced (Emsley 2011). About 30% of this total is used in iron ore refining operations prior to making steel (Emsley 2011), although this is decreasing as new steel processing techniques, such as hot metal desulfurization and ladle deoxidation, become more common. The remaining manganese is used to alloy steel. Most common steels have up to 1.0 wt % Mn (Lawcock et al. 2013). Manganese is considered a critical mineral because in its primary uses, particularly steelmaking, manganese cannot be substituted (NRC 2008). The addition of manganese increases the strength and hardenability of the steel (Lawcock et al. 2013; NRC 2008). Manganese serves other purposes in steelmaking, including acting as a deoxidizer, and combining with sulfur, phosphorus, and oxygen, to improve machinability of the steel and to reduce cracking during high-temperature rolling (Lawcock et al. 2013; IMnI 2014). High-strength, low-alloy (HSLA) steels, which contain 1.0–1.65 wt % Mn, have become relatively common in varied applications, with the manganese (and other alloying metals such as niobium and vanadium) used to decrease the carbon content while increasing the strength, weldability, and/or toughness (Davis 2001). In applications requiring high tensile strength, high toughness, and excellent wear resistance, such as gyratory and jaw crushers (IMnI 2014), the manganese content is increased to >11 wt % (Key to Metals AG 2010). In these instances, the steel is referred to as mangalloy. The manganese helps the steelwork harden as

William M. Cross, Professor, Materials & Metallurgical Engineering, South Dakota School of Mines & Technology, Rapid City, South Dakota, USA
Jon J. Kellar, Nucor Professor & Douglas W. Fuerstenau Professor, South Dakota School of Mines & Technology, Rapid City, South Dakota, USA

tensile forces cause a neck to form during elongation, greatly increasing the strength and elongation of such steels. In addition, the manganese inhibits the transformation of austenite to martensite. This causes the austenite phase to be metastable, and the transformation that can occur after impact can increase the surface hardness by up to three times. These properties make mangalloy difficult to machine, limiting its use. Manganese use is also significant in advanced high-strength steels, particularly twinning-induced plasticity (TWIP) steels (Chen et al. 2013). TWIP steels have 18%–30% Mn to stabilize austenite at room temperature. These steels offer up to two times the strength of mild steel, with ~5% lower density and increased energy absorption. This application is expected to lead to the use of considerable manganese in future vehicle manufacture as TWIP and HSLA steels are being used in FutureSteelVehicle construction, and in manganese dioxide cathode batteries in the electric version of the FutureSteelVehicle (Kilic and Ozturk 2014; WorldAutoSteel 2015).

Manganese is an important component of both primary (disposable) and secondary (rechargeable) battery cathodes (Gulf Manganese Corporation 2015a). For primary batteries, manganese dioxide serves as the cathode for the most common types of lithium-ion battery: CR-V3 or Li-Mn (Cadex Electronics 2015). The manganese dioxide cathode can absorb lithium ions and electrons formed at the lithium anode through an organic solvent with dissolved lithium salt to form $LiMnO_2$. Alkaline dry-cell batteries also use manganese dioxide. This type of battery was invented in the late 1950s, and more than 10 billion batteries per year are produced (Olivetti et al. 2011). These dry-cell batteries can also be designed to be rechargeable. A zinc anode and a manganese dioxide cathode are connected by a potassium hydroxide (alkaline) electrolyte.

With respect to aluminum alloys (3xxx series alloys), about 1 wt % Mn is added to wrought aluminum alloys to increase strength and allow strain hardening without decreasing ductility or resistance to corrosion (Woodward 2001). These alloys are typically used for cooking utensils and radiators, and so on, as they retain strength at elevated temperatures. Soda and beer cans typically contain about 1 wt % Mn, with the lids and bottoms having slightly less manganese. Increasing the manganese content creates what are termed *aluminum bronzes*. A representative aluminum bronze incorporating manganese is EN designation $CuAl_{10}Fe_3Mn_2$ with Al: 9–11 wt %; Fe: 2–4 wt %; Ni: <1.0 wt %; Mn: 1.5–3 wt %; Zn: <0.5 wt %; Si: <0.2 wt %; Pb: <0.02 wt %; and the remainder Cu (CDA 2004). Aluminum bronzes are valued for their corrosion resistance, particularly in seawater, leading to their use in several naval systems parts, particularly propellers for Arctic-travelling ships (LeGrand 2011). Other uses for aluminum bronzes include high-end guitar strings (Campus Five 2013), some coins (the Sacagawea dollar has 7 wt % Mn [U.S. Mint 2015]), and dental crowns (Eschler et al. 2003).

Less common uses of manganese include manganese ferrite ($Mn_xFe_{1-x}\,Fe_2O_4$) and manganese-zinc ferrites (Rashad 2006). These materials are often used in transformers and electromagnetic cores, particularly for frequencies <2 MHz (IMA 2011). Manganese compounds have been used to replace lead in unleaded gasoline (Gulson et al. 2006) and are critical nutritional components for aerobic life (Emsley 2011). Manganese-containing superoxide dismutase is present in nearly all eukaryotic mitochondrial cells and in bacteria and is necessary for the catalytic partitioning of toxic superoxides into gaseous oxygen or hydrogen peroxide (HHS 2012).

MINERALS OF ECONOMIC IMPORTANCE

Manganese can take on a variety of valence states, primarily from 2+ to 7+. Because of this speciation, many manganese minerals can form. As shown in Figure 1, water-stable manganese oxide minerals include pyrolusite (MnO_2, 4+ valence), bixbyite (Mn_2O_3, 3+ valence), hausmannite (Mn_3O_4, two 3+ and one 2+ valence), and pyrochroite ($Mn(OH)_2$, 2+ valence) (Hudson Institute of Mineralogy 2015). The prevalence of 2+ and 3+ valence states and their nearness on the periodic table makes iron and manganese similar in behavior, although manganese's higher oxidation states (leading to more minerals) and lower likelihood of forming sulfide minerals lead to separation of manganese from iron primarily into regions of higher solution oxidation potential. Other important manganese minerals include rhodochrosite ($MnCO_3$, 2+ valence), braunite (Mn_7SiO_{12}, six 3+ and one 2+ valence), cryptomelane ($(K,Ba)Mn_8O_{16}\cdot xH_2O$ or $K_2Mn_8O_{16}$, seven 4+ and one 3+ valence), and manganite (MnOOH, 3+ valence) (Hudson Institute of Mineralogy 2015). Rhodochrosite is the primary manganese mineral in about 33% of manganese deposits; braunite is primary in about 25% of deposits. Cryptomelane, manganite, and pyrolusite combine to be the predominant manganese mineral in a little more than 20% of all manganese deposits. Wad or bog manganese was used in ancient times for pigment and by the Romans for coloring glass. Wad is a poorly crystalline mixture of manganese oxides and hydroxides (Hudson Institute of Mineralogy 2015). Nsutite is a hydrated, gray-to-black, opaque manganese oxide of the formula ($Mn^{4+}_{(1-x)}\,Mn^{2+}_x\,O_{2-2x}(OH)_{2x}$, with x = 0.6–0.7 for Ghanaian, Greek, and Mexican nsutite, and x = 0.16 for manganoan nsutite from Ghana) (Zwicker et al. 1962).

GEOLOGICAL SETTING

Land-Based Resources

Figure 2 shows the distribution of the formation of manganese deposits throughout geological time. Volcanogenic manganese occurs in amounts too small to be seen in the figure. Manganese minerals were first deposited in large quantities at the start of the Paleoproterozoic era, coincident with the Great Oxidation Event and are generally associated with the Hamersley–Transvaal-type banded iron formations. The great Kalahari manganese field in South Africa, which contains most of the world's manganese deposits, is thought to be of sedimentary origin, occurring in shallow basins on the continental shelf. Initially, iron precipitated as an oxide or silicate, followed by silica, then manganese, likely as Mn^{4+} oxyhydroxide. Much of the manganese and associated metals transformed to Mn-Fe-Ca carbonates through diagenesis with organic carbon at relatively low Eh values. Two main types of deposit have been recognized, Mamatwan and Wessels. Mamatwan-type deposits make up about 97% of the field, typically have around 38% Mn with an Mn/Fe ratio of up to 10, ~5% SiO_2 (silicon dioxide), ~10% CaO (calcium oxide), and 3% MgO (magnesium oxide). Manganese minerals present in reasonable quantities include rhodochrosite, braunite, and manganite. In addition, the ore contains around 20% calcite, 5% magnesite, and 5% hematite. The remainder of the ore is a higher manganese oxide–type ore called Wessels. The manganese content of the Wessels-type ore is generally in excess of 45% and is mainly braunite, manganite, and hausmannite.

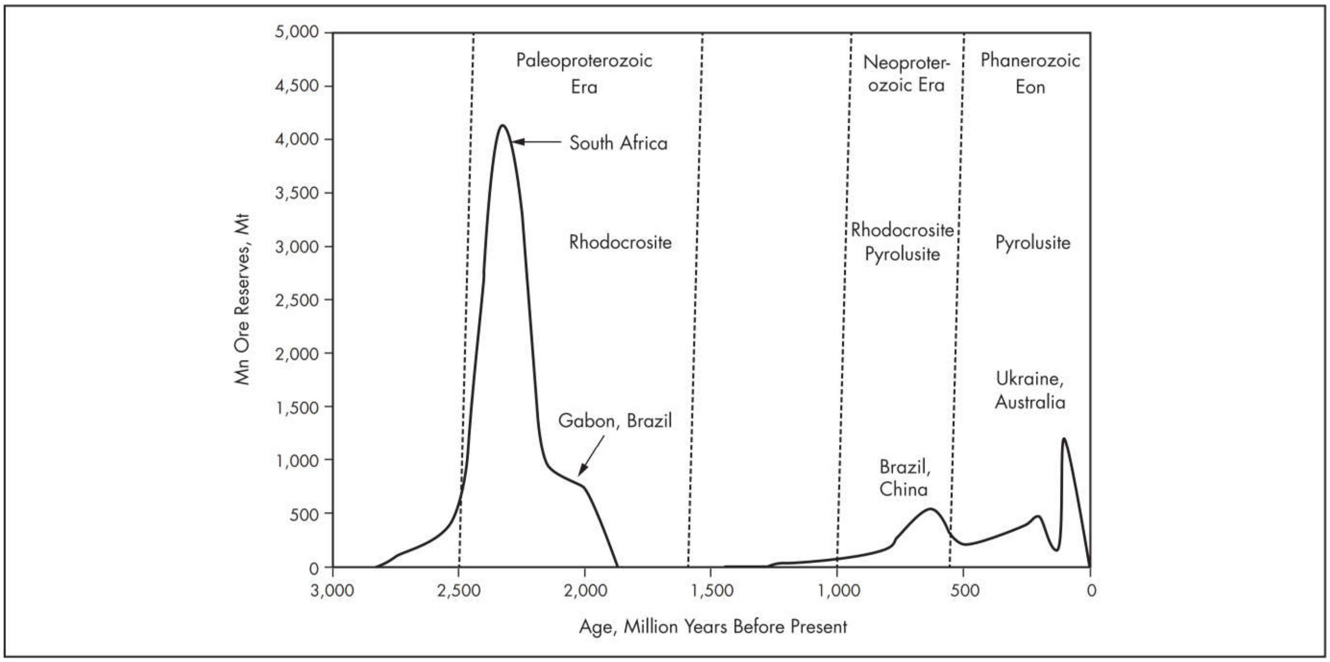

Source: Gutzmer and Beukes 2009

Figure 2 Manganese reserves as a function of time of deposit creation

The Mn/Fe ratio is typically 3–5, lower than in the Mamatwan ore. The calcite content can be 10%. The Wessels ore type is believed to have formed from hydrothermal alteration of the Mamatwan-type ore. Hydrothermal fluids, at 200°–250°C, entered the protore through cracks and leached the carbonate, calcium, magnesium, and silica. This resulted in the observed increase in manganese content and the transformation of the rhodochrosite to hausmannite.

In the late Paleoproterozoic (~2,000 million years ago), manganese deposits generally occurred as manganese-enriched black shale formations and formed as sedimentary deposits with low oxygen levels (<1 mL/L), with rhodochrosite formed by the interaction of organic carbon and Mn^{4+} oxyhydrides. These deposits typically have quartz, various clays, and pyrite as gangue minerals. Black shale–hosted deposits occur mainly in Moanda (Gabon), Azul (Brazil), and various areas of India and China. In addition to rhodochrosite (often calcium enriched), manganese is also present as manganese silicates and lower manganese valence oxides. These black shale–hosted protores have often transitioned to weathered deposits typical of a hot, humid lateritic process, leading to the oxidation of the manganese and loss of carbon dioxide and hydroxide. In these cases, the manganese composition is enriched from <30% Mn in the carbonate protore, some of which is still present at the lowest levels of the deposit, to high-grade oxide and silicate manganese ore deposits like those in Moanda, which in the processed portion contain about 40%–50% Mn as pyrolusite, with some manganite and cryptomelane. Moanda deposits contain about 8% silica, 7% alumina, and 5% iron as gangue.

Little manganese was deposited during the Mesoproterozoic. The deposition in the Neoproterozoic is correlated with the huge glaciation events of the Cryogenian period and decreased with the start of multicellular life in the Edicarian period. Similar to the early Paleoproterozoic Hotazel deposits, the manganese deposition correlates with banded iron formation, in this case, the Rapitan-type formations. For instance, at Mato Grosso do Sul (Brazil), cryptomelane is the most common mineral, followed by hematite, quartz, braunite, and pyrolusite, with some pyrite and a variety of other manganese and iron oxides and hydroxides.

The Phanerozoic eon deposits are of the shallow marine oolitic-type deposits. The primary manganese resources of this type are in Australia at Groote Eylandt and in Nikopol, Ukraine. As with the other manganese deposits, these are sedimentary in origin, usually in continental edge seas with low oxygen content. The manganese was deposited first as oxyhydroxide, was reduced to carbonates, and then weathered to form manganite, then pyrolusite and cryptomelane. For instance, at Groote Eylandt, pyrolusite and cryptomelane are the primary manganese minerals, while the primary gangue minerals are kaolinite, goethite, and quartz (Ostwald 1975).

Land-based deposits are usually mined as open-pit or open-cut operations (Moanda in Gabon; Mamatwan in South Africa; Bootu Creek, Groote Eylandt, and Woodie Woodie in Australia; Azul and Urucum in Brazil) with a few underground operations (Assmang and Wessels in South Africa).

Sea-Based Resources

Polymetallic sea nodules (PSNs) are not yet a productive source, but they have attracted a great deal of attention. The formation process of the nodules is different than the land-based manganese resources, yielding different manganese minerals and different accompanying minerals. PSN minerals form in two ways, hydrogenic and diagenetic precipitation. Initial nodule formation, at >4,000-m depths, is typically hydrogenic nucleation of vernadite (Mn^{4+}, Fe^{3+}, Ca^{2+}, Na^{+})$(O,OH)_2 \cdot n\ H_2O$. Bacteria may also be involved in the nucleation and growth of vernadite, $Mn_{1.4}$, $Fe_{0.6}$, $Ca_{0.1}$, $Na_{0.1}O_{1.5}OH_{0.5} \cdot 1.4H_2O$. Vernadite grows very slowly (1–10 nm/yr). As time passes, the nodules are eventually entrapped in porous sediment and the growth mechanism switches to produce todorokite $(K^+, Ca^{2+}, Na^+)_2(Mn^{4+}, Mn^{3+})_6O_{12}\cdot 3\text{–}4.5H_2O$, and with an empirical formula of $Na_{0.2}Ca_{0.05}K_{0.02}\,Mn^{4+}{}_4\,Mn^{3+}{}_2O_{12}\cdot 3H_2O$. Todorokite grows 10–100 times faster than vernadite. In some cases, birnessite $(K^+, Ca^{2+}, Na^+)(Mn^{4+}, Mn^{3+})_2O_4\cdot 1.5H_2O$ can form from todorokite.

PSNs occur throughout the oceans but are concentrated in the Pacific, including the Clarion-Clipperton zone (CCZ) between Mexico and Hawaii (15 kg/m^2 nodule density), the Peru Basin off the west coast of South America (10 kg/m^2 nodule density), near the Cook Islands in the southwestern Pacific Ocean (5 kg/m^2 nodule density), and Indian Ocean (5 kg/m^2 nodule density). The CCZ, Indian Ocean, and Cook Islands nodules have been reasonably well characterized. Manganese is relatively high in the CCZ and Indian Ocean nodules at about 28% and 24%, respectively, with 6%–7% Fe. The Cook Islands nodules have less manganese (~18%) and more iron (~16%) than CCZ and Indian Ocean nodules. The CCZ nodules have appreciable nickel, and the Indian Ocean nodules have nickel and copper, while the Cook Islands nodules are relatively enriched in cobalt and rare earth metals.

In addition to PSNs, ferromanganese sea crusts offer considerable potential as sources for manganese. These crusts form by the precipitation of vernadite and poorly crystalline ferric oxyhydroxide onto sediment-free rock surfaces, sea mounts, knolls, and plateaus. The crust formation in the Pacific Ocean is often similar to hydrogenetic PSN formation via cold water precipitation. In the Atlantic Ocean, crust formation is more often associated with hydrothermal vents. Such vents can reduce the metal concentration in the Atlantic Ocean crusts compared to Pacific Ocean Crusts. Once the crust is formed, other metals are adsorbed onto the crust, which can have specific surface areas up to 325 m^2/cm^3. Ferromanganese crusts are, therefore, enriched in metals, including cobalt, rare earth elements, nickel, and tellurium. The crusts typically contain around 20%–25% Mn regardless of location.

Largest Known Reserves

Current reserve estimates for manganese ores indicate that 150 Mt (million metric tons) of economically recoverable manganese exists in South Africa, primarily in the Mamatwan and Wessels formations. Ukraine has 140 Mt, much of that located in the Nikopol area; 97 Mt in Australia; 54 Mt in Brazil; 52 Mt in India; 44 Mt in China; and 24 Mt in Gabon. Mexico and Kazakhstan round out the list of countries with known significant reserves at 5 Mt each. Most of the world's manganese resources are in South Africa, generally estimated at up to 15 Bt (billion tons) of ore or 75% of the world's total land manganese reserves. Ukraine manganese reserves are estimated at 10% of the world total. In this chapter, the term *reserve* is not meant to denote a geologically proven quantity, and *reserve* and *resource* are used interchangeably, depending on usage in the cited document (Corathers 2015).

The reserves of PSNs are estimated to contain at least 6–7.5 Bt of manganese. Although the number of sea mounts, knolls, and plateaus is not well determined, the tonnage of manganese in ferromanganese crusts is estimated to be about 33% of the total estimated land manganese resources. Figure 3 shows the distribution of manganese reserves throughout the world.

LARGEST PRODUCERS

Manganese ore is processed in several countries, as shown in Figure 3. Production can be divided into large-scale production that is generally available to worldwide markets and small-scale production for local markets.

There are several commercial products. The main products are manganese ore (broken into classes by manganese content: 20%, 36%–39%, 42%, 44%, 46%, and >47% Mn), ferromanganese (broken into classes by carbon content: low carbon [<1% C], medium carbon [1%–2% C, 85% Mn], and high carbon [>2% C, 75% Mn]), silicomanganese, electrolytic manganese dioxide, and chemical manganese dioxide. Permanganate (potassium and sodium), manganese oxides other than dioxide, manganese sulfate, and manganese metal have lesser demand. Ore, from large-scale processing, is generally exported for conversion, usually to ferromanganese

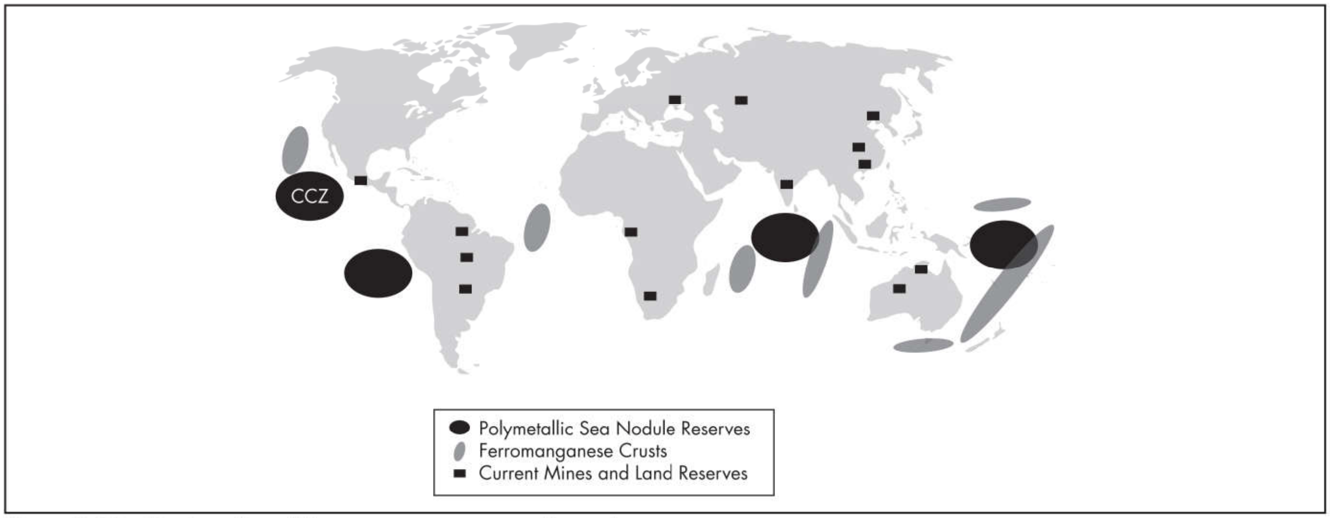

Figure 3 Distribution of world manganese reserves shown by type

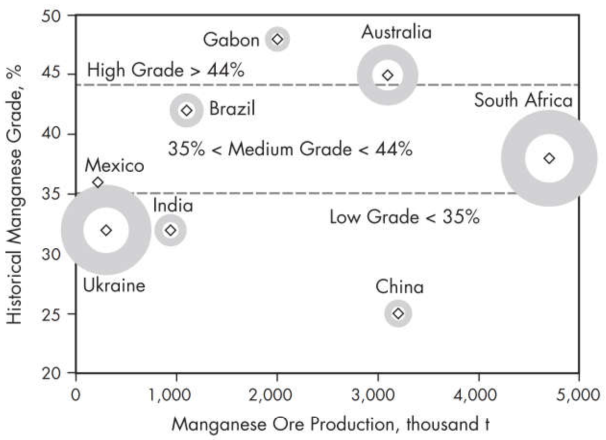

Note: The doughnuts indicate the proportional size of the countries' proven reserves. The diamonds represent manganese ore production. Mexico's reserves are smaller than the size of the diamond.

Data from Lawcock et al. 2013; Corathers 2015

Figure 4 Manganese ore production in 2014 by country as a function of historical grade of ore

or silicomanganese for steelmaking. Electrolytic manganese dioxide is used for battery cathodes, and chemical manganese dioxide is used for manganese ferrite production and for agricultural and chemical reaction purposes. Because of the variety of products, the manganese ore producers are discussed as related to the countries in which the mines exist, as shown in Figure 4.

Australia

Groote Eylandt Mining Company (GEMCO) is a subsidiary of South32 (which is currently "de-mergering" from BHP Billiton) and runs the primary processing facility for manganese at Groote Eylandt, Northern Territories, Australia, which opened in 1965 (South32 2017). The GEMCO facility can process 4–5 Mt/yr of ore (Wong 2011). The GEMCO ore is shipped to TEMCO, a wholly owned subsidiary in Tasmania, where the ore is transformed to high-carbon ferromanganese, silicomanganese, and sinter. OM Holdings operates the Bootu Creek mine, which opened in 2006. The ore processing facility is designed to process up to 1 Mt/yr. The Bootu Creek ore is typically shipped to China for ferroalloy (HCFeMn and SiMn) production. Pilbara Manganese, a wholly owned subsidiary of Consmin Ltd., runs the Woodie Woodie mine in Western Australia. The Woodie Woodie operation can process up to 1.5 Mt of ore per year. The processed ore is shipped directly to customers, often for specialty material production, as the ore has low silicon, phosphorus alumina, and iron content. Process Minerals International Pty Ltd. processes about 400,000 t of fines from the Woodie Woodie mine area (Mineral Resources Limited, n.d.).

Brazil

Vale S.A. is the primary manganese producer in Brazil, with ~70% of the Brazilian ore market. Vale product enters the market through a variety of wholly owned subsidiaries, including Vale Manganês S.A., Vale Mina do Azul S.A., and Mineracaõ Corumbaense Reunida S.A. Vale owns the Azul in Para and Urucum in Mato Grosso do Sul and makes ferromanganese (through Vale Manganês S.A.) in Minas Gerais and Bahia states (Gilroy 2014).

China

China produces more manganese than any other country. Most of this production is from imported ore that is used to produce refined manganese products, such as ferromanganese and electrolytic manganese metal. In about 2015, the main producers were Chongqing Tycoon Manganese Company Ltd. and Guangxi Dameng Manganese Industry Company Ltd. China imports manganese ore because the available domestic ore supply is unable to meet demand. Liaoning in Northeast China, Chongqing in Southwest China, Guangxi, Hunan, and Guizhou are the areas of China with the largest manganese reserves (Bloomberg 2015a, 2015b).

Gabon

Comilog (Compagnie minière de l'Ogooué), a subsidiary of Eramet, runs the Moanda mine. This mine produces very high-grade manganese ore. Typically, the ore is shipped after processing to various Eramet operations around the world, including Tinfos Jernverk in Norway for silicomanganese, ferromanganese alloys, and chemical manganese through Erachem Comilog in Belgium, the United States, Mexico, and China. The Moanda mine produced about 4Mt of ore in 2016 (Eramet 2018).

India

India, like China imports considerable manganese ore. MOIL (formerly Manganese Ore India Limited) produced about 51% of the manganese ore in India with 1.14 Mt of ore produced and was seeking to add four mines to its operations and to increase production by ~600,000 t/yr (Gundewar, 2014a, 2014b; Nagpur Pyrolusite 2015).

South Africa

The Mamatwan and Wessels mines (collectively, the Hotazel manganese mines) are primarily (74%) owned by South32 through South Africa Manganese, with the remainder owned by broad-based black economic empowerment investors (Gajigo et al. 2011). The processed ores are smelted by Metalloys at a facility near the mine in South Africa to make high- and medium-carbon ferromanganese and silicomanganese. Assmang Manganese (jointly managed by Assore Manganese and African Rainbow Minerals) also has mines in the Kalahari manganese field. Although much of the ore is exported after processing, Assmang operates four smelters (South32 2015; Kelly and Matos 2014).

HISTORICAL PRICE

The price of manganese ore, in constant-year dollars, tracks world manganese ore production to a certain extent but also has shown years of relative constancy, as shown in Figure 5. This relative constancy seems much less prevalent after 2010.

Mine production has been increasing steadily since the low of 6.4 Mt of manganese in 1999 to 17.4 Mt of manganese in 2014, with an increase of roughly 750,000 t of manganese per year. The price of manganese ore was relatively constant from 1994 through 2007 at about US$3.5/t in 2015 dollars, except for a small price shock in 2005 caused by increased demand for ferroalloys and increased transportation costs

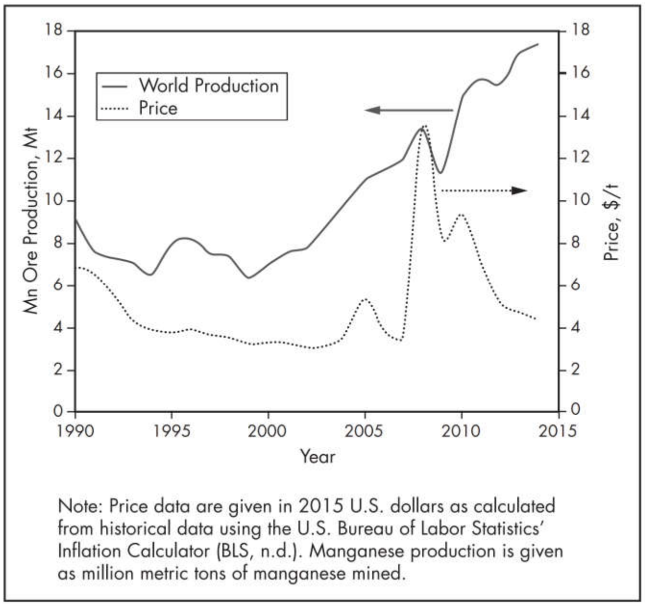

Data from Goonan et al. 2015; USGS 2016

Figure 5 Manganese production and price trends since 1990

(Matos and Carothers 2005). The price quadrupled in 2008, primarily because of two main factors, increased global consumption, mainly in China and India, and lower production in Brazil, China, and South Africa (Corathers 2008). Since the Great Recession of 2008–2009, the manganese ore price has begun trending back toward the previous long-term price. In other words, the market participants seem to have adjusted to the previous price fluctuations.

EXTRACTION

Traditionally, pyrometallurgical routes have been used to process manganese minerals to manganese-based materials, primarily ferromanganese and silicomanganese suitable for steelmaking. Beginning in the late-1930s in the United States, hydrometallurgical processing routes, both with and without pyrometallurgical pretreatment, have been investigated and/or commercialized. In this section, pyro- and hydrometallurgical processing routes are described, and recently developed methods for processing low-grade manganese deposits are discussed in more detail.

Beneficiation

A wide variety of manganese mineral beneficiation techniques have been utilized. For high-grade ores, beneficiation is often as simple as separating the fines after crushing and grinding. In this case, the manganese grade is increased by removing clay-type gangue particles (fines) that are often present in the sedimentary manganese deposits. For lower-grade ores, gravity separation, magnetic separation, and/or flotation are commonly performed (Pienaar and Smith 1992). Table 1 shows key separation parameters germane to the beneficiation of the various manganese minerals.

Pyrometallurgical Extraction

Pyrometallurgical extraction often follows a path similar to iron ore extraction. Specifically, the ore is crushed, ground, size fractionated, and beneficiated if necessary. For lateritic ores, the resulting concentrate is typically of a higher oxidation state, 4+, 3+ (Gordon and Nell 2013), including mineral classes such as manganese oxide (pyrolusite, cryptomelane, hausmannite) or silicate (mainly braunite) mineral with associated iron minerals. These types of concentrates are well-suited for preparing manganese for its main use in steelmaking. During smelting, the ore concentrate is mixed with coke (or other carbon form) and heated to at least 1,200°C (often 1,500°C for ferromanganese and 1,600°C for silicomanganese) in a reducing atmosphere. In many cases a flux, such as lime, silica, or calcite, is added to help remove impurities. Under these conditions, the high oxidation state manganese oxides are reduced to MnO (manganosite). A reduction reaction for pyrolusite is given in Equation 1. The MnO formed will then react with the coke to form manganese metal, as shown in Equation 2. Intermediate manganese oxides, such as Mn_2O_3, and Mn_3O_4, can also result.

$$MnO_{2(s)} + CO_{(g)} \rightarrow MnO_{(s)} + CO_{2(g)} \quad \textbf{(EQ 1)}$$

$$2MnO_{(s)} + C_{(s)} \rightarrow 2Mn_{(s)} + CO_{2(g)} \quad \textbf{(EQ 2)}$$

Three primary products are formed for use in steels: silicomanganese (SiMn), high-carbon ferromanganese (HCFeMn), and refined ferromanganese (refined FeMn). The most commonly used (~55%) smelter product is silicomanganese. Silicomanganese contains 65%–70% Mn, 18%–20% Si, and 1%–2% C, with the remainder primarily iron and is usually used to deoxidize steel. The feed material is typically a mix between manganese ore and slag from high-carbon ferromanganese production. Smelting is often performed in a submerged electric arc furnace with the smelting temperature >1,600°C to allow the ore and the ferromanganese slag to melt fully, thereby yielding a high silicon content and low MnO content in the slag. ASTM Standard A483-10 defines silicomanganese compositions. Three grades are distinguished by their carbon and silicon contents. The ASTM standard requires 65%–68% Mn for all grades. For example, Eramet Comilog (2013) specifies P < 0.17% and S < 0.03%. About 75% of the SiMn manufactured goes to steel mini mills. After melting, the SiMn is tapped and cast into billets that are then crushed. The crushed SiMn is typically sold as the bulk crushed alloy. As an example, Eramet Comilog produces SiMn in France and Norway and sells the material in three size ranges (20–80 mm, 10–50 mm, and 3–25 mm) as a bulk material packaged in big bags with other packaging available on request.

For HCFeMn, ASTM 99-03 (2014) indicates that the Mn concentration should be between 74% and 82% depending upon grade, <7.5% C, <1.2% Si, <0.35% P, and <0.05% S. HCFeMn is mainly 85% Mn and is used by integrated steel mills, with the balance used by mini mills. In general, making HCFeMn is similar to making SiMn. Submerged arc furnaces are generally preferred, although blast furnaces can be used. Coke and limestone are added to lower the oxidation potential and to provide a slag former, respectively. The temperature can be a little hotter than that used in silicomanganese production, up to 1,800°C. The feed is typically manganese ore, beneficiated as necessary to achieve >40% Mn, with preheating and oxygen enrichment when blast furnaces are used. Slag characteristics are very important to the performance of the furnaces. Fines should be avoided in submerged electric arc furnaces, as the fines have a tendency to disrupt the flow of carbon monoxide and carbon dioxide (CO and CO_2) through the burden. When fines are to be used, they must be agglomerated and

Table 1 Key separation parameters for manganese minerals

Mineral	Formula	Density, g/cm^3	Reference	Magnetic Susceptibility, 10^{-3} cm^3/g	Reference	Point of Zero Charge pH	Reference
Land-Based Mineral Separation							
Braunite	Mn_7SiO_{12}	4.7–4.8	Hudson Institute of Mineralogy 2015; Drzymala 2007	<1; 0.025–0.5*	Taneja and Garg 1993; Rosenblum and Brownfield 2000	—	—
Cryptomelane	$K_2Mn_8O_{16}$	4.4	Drzymala 2007	0.3–0.6*	Rosenblum and Brownfield 2000	<3, 1.7–2.1	Kosmulski 2009
Hausmannite	Mn_3O_4	4.77–4.85	Todd 2010; Hudson Institute of Mineralogy 2015	0.5–0.76	Drzymala 2007	<5, 6.5, >10	Rosenblum and Brownfield 2000; Drzymala 2007; Tan et al. 2008; Kosmulski 2009
Manganite	MnO(OH)	4.3–4.4	HHS 2012; Drzymala 2007	0.36–0.5	Drzymala 2007	6.3, 7.4	Rosenblum and Brownfield 2000; Kosmulski 2009
Pyrochroite	$Mn(OH)_2$	3.26	Drzymala 2007	—	—	7	Kosmulski 2009
Pyrolusite	MnO_2	4.7, 5.04–5.08	Todd 2010; Hudson Institute of Mineralogy 2015	0.30.48	Drzymala 2007	4–8, 7.2	Kosmulski 2009; Tan et al. 2008
Rhodochrosite	$MnCO_3$	3.7	Hudson Institute of Mineralogy 2015; Drzymala 2007	1.31–1.34	Drzymala 2007	6–10.5	Kosmulski 2009
Sea-Based Mineral Separation							
Birnessite	$(K,Ca,Na)(Mn)_2O_4 \cdot 1.5H_2O$	3.0	Drzymala 2007	—	—	1–1.6	Tan et al. 2008
Todorokite	$Na_{0.2}Ca_{0.05}K_{0.02}Mn_6O_{12} \cdot 3H_2O$	3.7	Drzymala 2007	—	—	3.2, 3.4–4, 3.8	Tan et al. 2008; Kosmulski 2009

*Value given is amperage needed to attract the mineral in a modified Frantz isodynamic separator.

sintered. This can be helpful because this process can be used to pre-reduce the manganese oxides, lowering the coke and temperature requirements.

When SiMn and HCFeMn are made near each other, high-manganese slags are often produced for feed to the SiMn smelter. The high-manganese slag contains 30%–40% Mn, 2%–5% MgO, 10%–30% Al_2O_3 (aluminum oxide), 15% CaO, and 25%–30% SiO_2. Manganese ores containing <40% Mn can also be used, and these are typically smelted to produce low-manganese slag. In these cases, and for most discarded slags, the manganese is less than 20%, with recovery typically >85%. Other slag components include up to 8% MgO, 10% Al_2O_3, 35% CaO, and 30% SiO_2. Again, the HCFeMn is cast, crushed, and sold as the bulk crushed alloy. Eramet Comilog sells this material in the same size and manner as SiMn.

Refined FeMn is also called low- or medium-carbon FeMn. Grades as specified by ASTM A99-03 (2014) are 80%–85% Mn for medium-carbon FeMn and 80%–90% Mn (depends on the grade) for low-carbon FeMn. Medium-carbon FeMn has less than 1.5% C, while low-carbon FeMn contains <0.75% C (depends on grade). The phosphorus and sulfur are slightly lower after refining, <0.3% P in both low- (depends on grade) and medium-carbon FeMn and <0.02% sulfur in both types of refined FeMn. The amount of silicon varies between the different grades of refined FeMn. Refining can be performed by oxidation of some of the carbon in the HCFeMn. Silicothermic reduction can also be used. In silicothermic reduction, SiMn is mixed with manganese ore and lime or a high-manganese slag to reduce the MnO and form Mn. The lime is used to reduce the activity of the silica to force the MnO reduction to produce more Mn. Integrated mills use about 70% of the refined FeMn, with much of the rest procured by specialty steel manufacturers for production of stainless steel and HSLA steels. Eramet Comilog sells this material in the same size and manner as SiMn.

A manganese life-cycle assessment was recently performed by the International Manganese Institute. Typical manganese production methods release about 6 kg CO_2 equivalents per 1 kg of manganese alloy. In addition, 3 g ethane equivalent, 45 g SO_2 equivalents, and 9.6 g particulate matter are released per kilogram HCFeMn. Except for particulate matter, electricity generation is responsible for 60%–80% of these emissions (IMnI 2016).

An example of a modern smelter operation is that proposed by Gulf Minerals in West Timor, Indonesia (Gulf Manganese Corporation 2015b). Indonesia has considerable manganese reserves, both on land and as sea nodules/ferromagnetic crusts (Cunningham 2015); however, little exploitation of these reserves has occurred. The Timor smelter is expected to use high-quality local manganese ore, as Indonesian law limits the exportation of unprocessed ore. The ore to be used in Timor has a low iron content (~2%) as well as low phosphorus and sulfur (see Figure 6). The ore is to be jigged to remove the low-density silica and clay minerals and increase the manganese grade. After jigging, the manganese concentrate, iron ore, metallurgical coal, and limestone will be added to the partially submerged electric arc furnace to make the HCFeMn. Eight furnaces are planned, which will require 64 MW of power, necessitating a dedicated coal-fired power plant at the smelter site. The furnaces will be tapped every 90–100 minutes. When fully completed, 290,000 t of high-manganese ore will be processed per year, leading to 155,000 t of HCFeMn. The smelting requires ~0.944 t of coal, 0.337–0.502 t of limestone, and 0.212 t of iron ore per ton of HCFeMn. For the desired amount of HC FeMn, ~145,000 t of

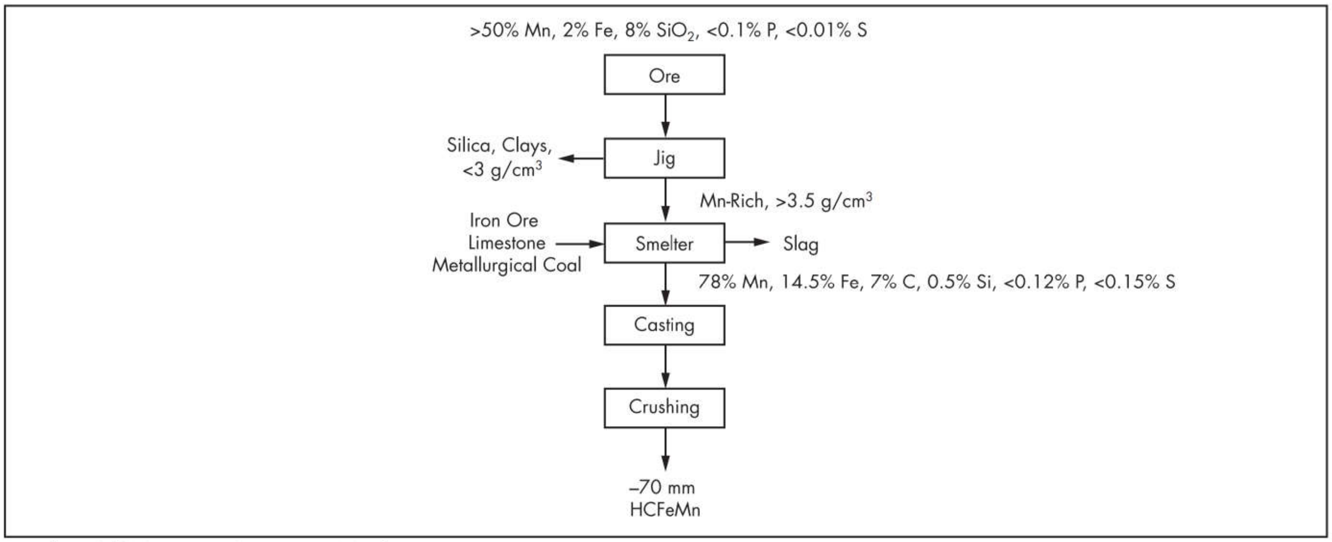

Data from Gulf Manganese Corporation 2015b

Figure 6 Flow sheet for the Gulf Minerals high-carbon ferromanganese plant in West Timor, Indonesia

metallurgical coal are required, along with ~50,000–75,000 t of limestone and 30,000–35,000 t of iron ore. The HCFeMn will be exported, with ~50% to Europe, 25% to Japan, with smaller amounts to Korea and China.

Hydrometallurgical Extraction

The U.S. Bureau of Mines conducted extensive laboratory and pilot-scale investigations in the 1930s and operated a large experimental plant at Boulder City, Nevada (United States), during 1942–1946 and a pilot plant near Oacoma, South Dakota (United States), from 1944–1946. The first commercial hydrometallurgical plant was completed by Electro Manganese Corporation in Knoxville, Tennessee (United States) in 1939. These facilities produced electrolytic manganese metal (EMM) by reduction roasting of pyrolusite to MnO and leaching of the MnO with dilute sulfuric acid. Subsequent installations were built by Union Carbide's Metals Company (later Elkem Metals Company) in Marietta, Ohio; Foote Mineral Company in New Johnsonville, Tennessee; and American Potash Corporation (later Kerr-McGee Chemical Corporation) in Hamilton, Mississippi, and Henderson, Nevada (all in the United States). EMM was initially produced at all of these locations, except Henderson, where only electrolytic manganese dioxide (EMD) was produced as an anode deposit. Eventually, Union Carbide and Foote also produced EMD for use mainly in dry-cell batteries (T.P. McNulty, personal communication).

Flow sheets varied and were periodically upgraded, but reduction roasting was accomplished either in enclosed furnaces or open heaps with natural gas or propane introduced through a supporting grid, producing a reducing environment within the heap. Following solid–liquid separation, the filtrate was treated with sulfide ion or hydrogen sulfide gas to precipitate heavy metals. The clarified filtrate was electrolyzed. Anodic deposition of EMD was on graphite plates that were manually stripped, while water-cooled tubing served as the cathode. Cathodic deposition of EMM was enabled by operating at an elevated electrolyte temperature with perforated anodes to increase the current density on the anode surface and retard deposition of EMD. Diaphragms were used to isolate the electrodes that were not being harvested (e.g., the anodes, in the case of EMM production). The plants previously mentioned had aggregate capacities of about 12,000–30,000 t annually of EMM or EMD. During the early-1980s, EMD producers struggled to make a product that had a 3-year battery shelf life, whereas modern dry-cell batteries typically have a 10-year shelf life. The improvements are attributable to advancements in electrolyte purification, product grinding and classification, process control, and quality assurance and quality control procedures. The original technologies suffered from high labor intensity, largely due to small cathode blanks for EMM and small graphite anodes for EMD. The graphite anodes were fragile and were gradually destroyed by oxidation (from evolved oxygen gas) and by operators being too aggressive with mallets used to dislodge the brittle deposit (T.P. McNulty, personal communication).

Hydrometallurgical processing has been accomplished in two ways: either a hybrid pyro-hydrometallurgical route or a direct hydrometallurgical route can be taken.

Pyro-Hydrometallurgy

In the combined pyro-hydrometallurgy treatments of manganese ores, two main types of pyrometallurgical pretreatments are used. The first of these is sulfation roasting of pyrolusite to form manganese sulfate, and the second is calcination of rhodochrosite to a manganese oxide.

For the sulfation roast, pyrolusite ore is heated in the presence of SO_2 (sulfur dioxide) gas or in the presence of a sulfate chemical such as sulfuric acid or ammonium sulfate. Roasting with SO_2 can be accomplished at relatively low SO_2 partial pressure and moderate temperature. For many manganese ores, too high a partial pressure can lead to increased sulfation of iron oxides, while too high a temperature (>~525°C) leads to transformation of the MnO_2 to bixbyite (Mn_2O_3), which is less amenable to sulfation, thereby increasing the difficulty of leaching. Manganese sulfate is quite soluble in water (>35% at 20°C, decreasing to 10% at 140°C), and the rate and equilibrium extraction can be increased with temperature. Decreasing the pH does not appreciably change the extraction. With sulfuric acid roasting, the roasting can be accomplished at much lower temperatures than roasting with SO_2 gas. Roasting temperatures as low as 150°–200°C can yield >90% extraction of manganese after one hour of ambient temperature leaching (Güler et al. 2008; Zhang et al. 2013; Guo et al. 2009).

In the calcination of rhodochrosite, the ore is heated to drive off the CO_2 gas, typically at temperatures of 800°C or greater (You et al. 2015). At these temperatures in an air atmosphere, the MnO formed oxidizes to MnO_2, which is then cooled and subject to leaching. Thermal reduction of manganic oxides to MnO, as practiced in the United States by Union Carbide and Kerr-McGee Chemical Corporation, was accomplished at moderate temperatures in a reducing atmosphere created by incomplete combustion of natural gas or propane.

Hydrometallurgy

Leaching. The leaching of manganese ores and pyrometallurgically treated concentrates has been studied fairly extensively. As can be seen from examination of Figure 1 and similar Pourbaix diagrams (Veglio et al. 2001), manganese oxides are subject to leaching by lowering the pH and Eh to yield Mn^{2+} ions. Solubility product (K_{sp}) data are available for a few manganese compounds and can be calculated from various databases (Gustafsson 2015; Pourbaix 1974): $MnCO_3$, $K_{sp} = 1.8 \times 10^{-11}$; $Mn(OH)_2$, $K_{sp} = 1.5 \times 10^{-13}$; and MnS, $K_{sp} = 3.7 \times 10^{-15}$ (the preceding calculations were performed with data from the Minteq database [Gustafsson 2015]). Manganese carbonate leaching is assisted by carbonate ions, because at pH <5–6, most of the carbonate will react to form carbon dioxide, reducing the carbonate ion activity and hence causing the manganese activity in solution to be high. Thus, the manganese extraction will be relatively high at these mild pH values. For manganese hydroxide, similar to manganese carbonate, fairly mild pH values allow high manganese ion activity to be achieved. For typical ore constituents, the chemical reactions are slightly more complicated than for the simple carbonate and hydroxide minerals discussed. Also, the manganese solubility is a function of the oxygen fugacity, in addition to the temperature and pH. For pyrolusite, a simple leaching reaction can be written:

$$MnO_{2,s} + 2H^+_{aq} \rightarrow Mn^{2+}_{aq} + H_2O + 0.5O_{2,g} \qquad \textbf{(EQ 3)}$$

The equilibrium constant for Equation 3 is 1.02 (calculation performed with data from the Minteq database [Gustafsson 2015]). Therefore, while the reaction proceeds to the right, low pH and/or low oxygen pressures are needed to achieve significant manganese extraction. For instance, when leaching in air, a pH of 1.67 is needed to achieve a manganese concentration of ~55 ppm. Parc et al. (1989) have written similar equations for several manganese minerals, including cryptomelane, lithiophorite, nsutite, birnessite, manganite, and rhodochrosite. A similar reaction to Equation 3 using manganese carbonate rather than manganese oxide has an equilibrium constant of ~2,000 and gives a manganese activity of 0.001 at pH 5.9.

Because of the preceding considerations, more complicated hydrometallurgical methods have been developed. In general, the methods have been primarily aimed at leaching pyrolusite with lixiviants in addition to hydrogen ions. For instance, in methods somewhat similar to sulfation roasting, SO_2 gas or other sulfur-based reductants, such as dithionate or sulfite, are used, usually with sulfuric acid. Sulfur dioxide is oxidized to sulfate and dithionate, while the manganese is reduced and forms Mn^{2+} in aqueous solution. Ferrous sulfate has also been used to leach pyrolusite, with the product being manganese sulfate and various ferric salts, and the composition of these salts depends on the amount of acid available. With enough excess sulfuric acid, ferric sulfate is formed.

For low-manganese-content resources, lower cost methods have been studied to leach manganese (e.g., Zhang and Cheng 2007; Chow et al. 2010, 2012, 2013). Many of these methods revolve around the use of organic, primarily sugar-based, reductants in sulfuric acid solution (Beolchini et al. 2001; Ismail et al. 2004; Furlani et al. 2006; Su et al. 2008, 2009; Lasheen et al. 2009). These organic reductants include glucose, sucrose, lactose, sawdust, waste tea, molasses, glycerin, plant leaves, and several varieties of fungi and microbes. The organic reductants are generally chosen to reduce the cost of leaching with the cost reduction meant to offset the loss in value associated with the lower content of valuable metal. Typically, sulfuric acid is used for leaching, although hydrochloric and nitric can also leach manganese minerals.

Pressure leaching has been explored for nodules and crusts, but this is typically performed to remove non-manganese value, and manganese extraction is low.

Recovery from solution. Once manganese ions have been leached from the ore, the aqueous solution needs to be concentrated and purified, and the manganese recovered in a suitable form. How this is accomplished is dependent on the other ions that are leached along with the manganese ions. For oxide-based manganese ores, the typical gangue minerals include alumina, quartz and hematite, and clays, such as kaolinite. For the carbonate-based ores, calcite, siderite and mixed carbonates, such as dolomite, and mangano calcite can be present, along with quartz and clays. Other metallic cations, such as zinc, arsenic, cobalt, and cadmium, are often present in relatively small amounts in manganese ores but are often sufficient to make these metals the primary recovery target in nodules and crusts. In many cases, useful methods for recovery from solution arise by reversing the leaching processes, as revealed by the use of Pourbaix diagrams (see Figure 1). In these cases, solution purification can be achieved by raising the pH. At 25°C, one expects, thermodynamically, that hydroxides will precipitate from solution in the following order: Fe^{3+}, Al^{3+}, Cu^{2+}, Zn^{2+}, Fe^{2+}, Co^{2+}, Mn^{2+}, Mg^{2+}, and Ca^{2+}. For instance, when testing an Arizona manganese ore for American Manganese, Kemetco Research found that raising the pH of the pregnant leach solution (PLS) from ~1 to ~5.6 removed ~98% of the Al, >94% of the As, >90% of the Cu, 99.7% of the Fe, 89% of the Si, and 57% of the Zn in solution, while the manganese content was reduced ~2% and the cobalt concentration was reduced about 11.5% (Chow et al. 2010, 2012, 2013). The hydroxide-treated PLS was then subject to sulfide precipitation primarily to remove the remaining cobalt and zinc. The thermodynamic order of removal is expected to follow the trend Cu, Cd, Zn, Co, Fe, Mn. Overall, at least 90% of Al, As, Co, Cu, Fe, Si, and Zn were removed sufficiently to yield a suitable feed for further processing of the PLS. The loss of manganese was 2.4%, while K, Ca, Mg, and Na ion concentrations were constant or increased. This type of processing is useful to produce a final leach solution that is primarily manganese in terms of its metal content. In the Kemetco Research data previously discussed, Mn^{2+} makes up about 80% of the metal value after hydroxide and bisulfite precipitations.

Precipitation of manganese carbonate is a common method for recovering manganese solution. Precipitation requires raising the pH of the leach solution and adding carbonate ions. Carbonate ions become the predominant species at pH ~9.5. Sodium or ammonium carbonate can be used, typically, in approximately equal stoichiometry with the manganese ions. Manganese carbonate is typically recovered as a precursor to making sintered-FeO/MnO feed materials for FeMn manufacture.

Another very common precipitation is the formation of MnO_2 as either EMD or chemical manganese dioxide (CMD). To precipitate EMD or CMD, the reaction must be performed with an oxidant (Zhang et al. 2002). The chosen oxidant must be sufficient to account for the potential of the MnO_2 reaction of 1.224 V (Pourbaix 1974). Oxidants that have been used include ozone–oxygen gas mixture, sulfur dioxide–oxygen, chloric acid, and hydrogen ions.

The primary difference between EMD and CMD materials is the purity needed. The EMD material is used in batteries and usually needs a higher purity than the CMD material, which is used for ferrites. EMD is often packaged as powder in 25- or 50-kg net paper or plastic/composite bags from China, or 50-lb bags or 3,000-lb super sacks in the United States by Tronox. CMD is packaged similarly to EMD in 25- or 50-kg woven bags, typically with an inner liner.

Manganese metal is the result of electrowinning PLSs. The electromotive force (emf) for the manganese metal-manganese 2+ ion couple is –1.18 V (Pourbaix 1974). As this emf value is quite low, as evidenced by Figure 1 in which manganese metal is not stable in water, the concentration of all ions having greater emf than –1.18 V should be kept low to keep the current efficiency high. Cobalt has the greatest negative effect, followed by nickel, copper, zinc, silicon, and ferrous iron. American Manganese, in their low-grade manganese process, investigated electrowinning of manganese metal from the purified PLSs. Current efficiencies of >65% were achieved using a Pb-Ag anode and a stainless-steel cathode. The feed solution contained 30–40 g/L Mn, 130–150 g/L ammonium sulfate, 1–2 g/L sodium sulfite, 350 A/cm^2 current density, feed pH 6.2, and a flow rate of 2 mL/min. Deposition was performed for 18–24 hours at 35°C. A small amount of SO_2 gas was used to improve current efficiency, primarily through conversion of γ-Mn to a fine-grained α-Mn. The grade of the plated manganese achieved was greater than 99.5% Mn. One final key to achieving the most efficient electro-deposition is the avoidance of forming MnO_2 at the anode. American Iron and Steel type 316 stainless steel seems to work best for reducing manganese dioxide formation. Temperatures exceeding 36°–38°C also reduce the current efficiency of the manganese electrowinning. These conditions are essentially identical to those developed by the U.S. Bureau of Mines and commercialized as discussed earlier. EMM is often produced as powder or flakes that are sold in 1,000-kg big bags, although smaller bag sizes are often available.

The recovery of manganese from aqueous solution using solvent extraction has also been well studied (Zhang and Cheng 2007). The extraction of manganese has been accomplished using phosphoric acid–based (bis[2-ethylhexyl] hydrogen phosphate, DEHPA, D2EHPA, or HDEHP), phosphinic acid–based (Cyanex 272), phosphonic acid–based (PC-88A/Ionquest 801), and carboxylic acid–based (Versatic 911) extractants. Acids used to alter the solution pH include sulfuric, hydrochloric, and nitric acids. The general solvent extraction equation can be written as follows:

$$\mathrm{mMn^{2+} + nm(H_2A_2)_{organic} \leftrightarrow [\{Mn(H_{2n-2}A_{2n})\}_m]_{organic} + 2mH^+} \qquad \textbf{(EQ 4)}$$

Usually, m = n = 1 is assumed for charge balance and simplicity considerations. However, while in most of the literature m = 1, n has been found typically to have been between 2 and 3. This indicates that some neutral extractant must be part of the extractant complex and that the coordination structure of the complex needs to be considered to better understand the extraction process. Extraction of manganese by DEHPA in sulfuric acid solutions was studied and gave a pH_{50} (the pH at which 50% of the metal ion is extracted) of ~2.7 when performed in the presence of calcium and magnesium. Under these conditions, the manganese is generally not extracted as well as zinc, but it is better than cobalt, copper, and nickel. With PC-88A, manganese extraction varies between sulfate and chloride media. The pH_{50} in sulfate media was found to be 3.2, but shifts to 2.6 in chloride media. With Cyanex 272, the pH_{50} in sulfate media was 4.6. For many systems, the extraction order has been found to be DEHPA > PC-88A > Cyanex 272. Manganese solvent extraction is often performed in the context of separating manganese from zinc, and cobalt, and nickel. Combinations of extractants have become more common recently. This trend is driven by the synergistic nature of the combined extractants.

Low-grade manganese value processing. As the high-grade ores become depleted, new processes for the extraction of low-grade deposits will be of great importance. One example is the process developed by Kemetco Research for American Manganese for their Artillery Peak (Arizona, United States) deposit. Figure 7 shows an outline of the flow sheet developed. Such a hydrometallurgical approach is likely to have considerable cost savings compared to conventional pyrometallurgical processes. One of the keys to this new process is the efficient destruction of dithionate. This method is reasonably versatile, as EMD, CMD, or feed for SiMn and FeMn can be produced with small changes in the process, mostly in the electrowinning circuit (Chow 2010, 2012, 2013).

SUMMARY

Manganese is considered a strategic metal and is essential for making many specialty steels. As >90% of manganese produced is used in steelmaking, the production and consumption of manganese should follow the basic trends expected for steel (Papp et al. 2007), with ~2%–5% annual growth through 2030. New uses related to batteries for electronic devices are also expected to become a greater driver for manganese consumption. Figure 8 shows a flow sheet for manganese materials. Currently, ~94% of manganese ore is processed pyrometallurgically. Of that, 75% is consumed in steel production, 15% ends up as slag from steelmaking, and 10% is used in foundries and welding applications. For the 75% used for steels, 55% goes to silicomanganese production, 35% to high-carbon ferromanganese production, and 9% to refined ferromanganese. The primary consumers of SiMn are mini mills, while integrated steel mills are the main consumers of the ferromanganese alloys. Hydrometallurgically produced manganese is primarily consumed as EMD for batteries and CMD for ferrites, agricultural chemicals, and dietary supplements and pure manganese metal. Approximately 50 new mines or mine

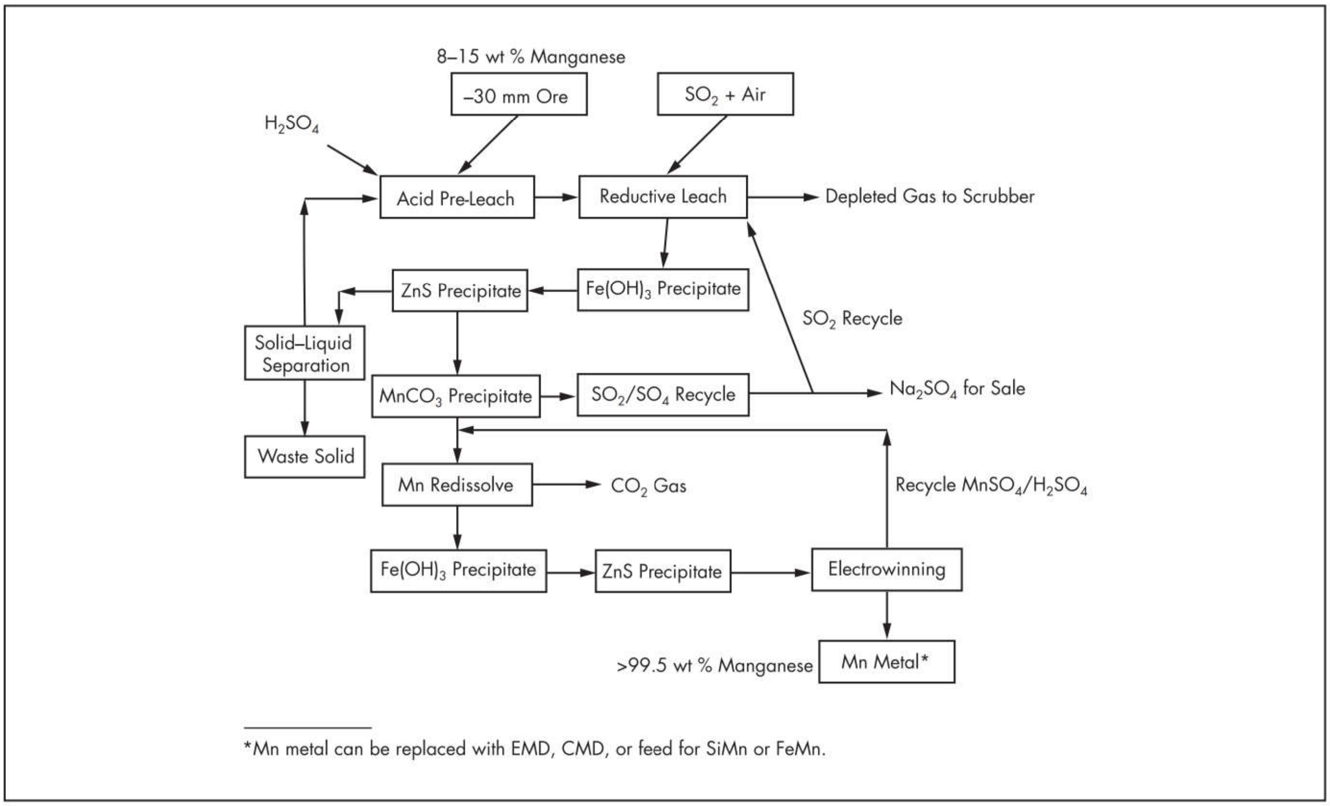

*Mn metal can be replaced with EMD, CMD, or feed for SiMn or FeMn.

Source: Chow et al. 2010, 2012, 2013

Figure 7 Flow sheet for the Kemetco Research American Manganese/Artillery Peak process

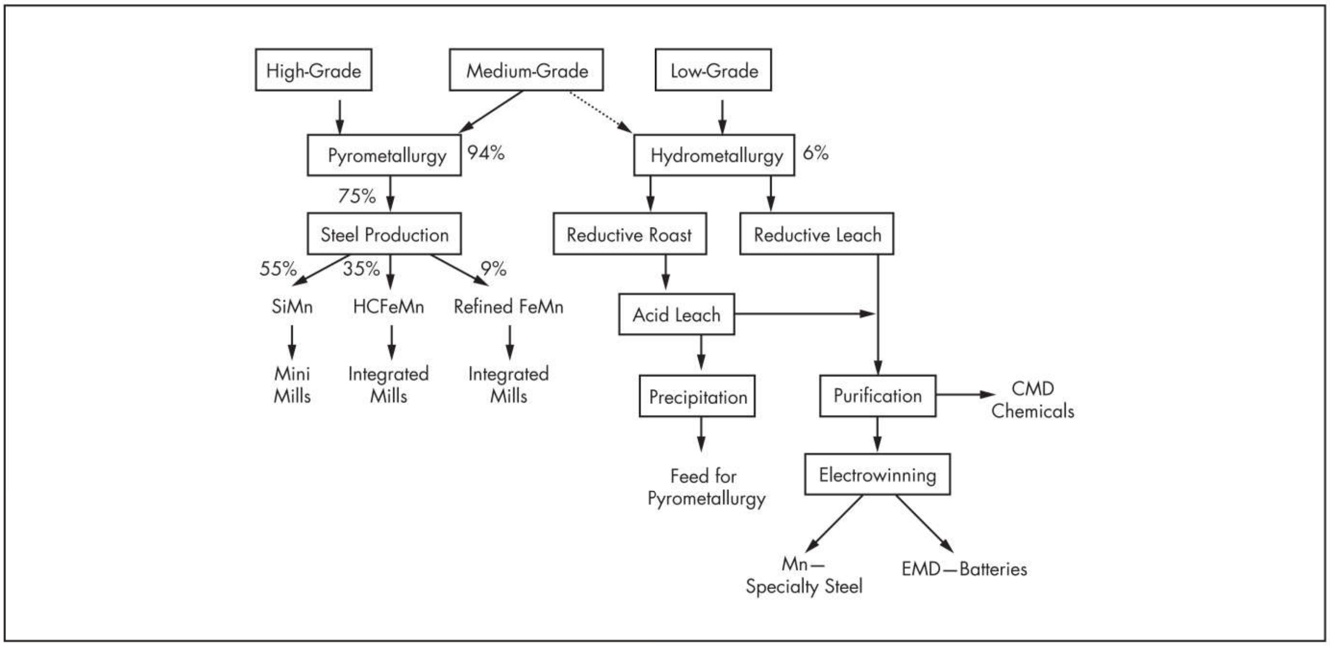

Data from Lawcock et al. 2013; Chow et al. 2012, 2013

Figure 8 Flow sheet for manganese production from ore

expansions were in development at the height of the manganese price bubble from 2009 to 2012 (Corathers 2014). The return of the manganese price to historic levels will likely cause many of the new mines to be placed on standby until most of the high-grade ores are depleted, at which point they may again be commercially viable, depending upon the utilization of sea nodules and ferromanganese crusts.

REFERENCES

ASTM A99-03. 2015. *Standard Specification for Ferromanganese.* West Conshohocken, PA: ASTM International.

ASTM A483-10. 2015. *Standard Specification for Silicomanganese.* West Conshohocken, PA: ASTM International.

Beolchini, F., Papini, M.P., Toro, L., Trifoni, M., and Veglio, F. 2001. Acid leaching of manganiferous ores by sucrose: Kinetic modelling and related statistical analysis. *Miner. Eng.* 14:175–184.

Bloomberg. 2015a. Chongqing Tycoon Manganese Industry Co. Ltd. Company profile. www.bloomberg.com/profiles/companies/0774928D:CH-chongqing-tycoon-manganese-industry-co-ltd. Accessed August 2015.

Bloomberg. 2015b. Metals and Mining: Company overview of Guangxi Dameng Manganese Industry Co., Ltd. www.bloomberg.com/research/stocks/private/snapshot.asp?privcapid=53303562. Accessed August 2015.

BLS (U.S. Bureau of Labor Statistics). n.d. Inflation calculator. www.bls.gov/data/inflation_calculator.htm. Accessed August 2015.

Cadex Electronics. 2015. Battery University—BU-205: Types of lithium-ion. Richmond, BC: Cadex Electronics. www.batteryuniversity.com/learn/article/types_of_lithium_ion. Accessed August 2015.

Campus Five. 2013. Guitar string composition and swing guitar [blog]. Jonathan Stout and his Campus Five. www.campusfive.com/swingguitarblog/2013/5/16/guitar-string-composition-and-swing-guitar.html. Accessed August 2015.

CDA (Copper Development Association). 2004. *Copper and Copper Alloys: Compositions, Applications and Properties.* Publication 120. Hertfordshire, UK: Copper Development Association.

Chalmin, E., Vignaud, C., Salomon, H., Farges, F., Susini, J., and Menu, M. 2006. Minerals discovered in paleolithic black pigments by transmission electron microscopy and micro-X-ray absorption near-edge structure. *Appl. Phys. A* 83:213–218.

Chen, L., Zhao, Y., and Qin, X. 2013. Some aspects of high manganese twinning-induced plasticity (TWIP) steel: A review. *Acta Metall. Sinica* 26:1–15.

Chow, N., Nacu, A., Warkentin, D., Aksenov, I., and Teh, H. 2010. *The Recovery of Manganese from Low Grade Resources: Bench Scale Metallurgical Test Program Completed.* IRAP Project no. 712681. Richmond, VA: Kemetco Research.

Chow, N., Nacu, A., Warkentin, D., The, H., Aksenov, I., and Fisher, J.W. 2012. New developments in the recovery of manganese from lower-grade resources. *Miner. Metall. Process.* 29:61–74.

Chow, N., Nacu, A-C., Warkentin, D., and Fisher, J.W. 2013. Processing of manganous sulphate/dithionate liquors derived from manganese resource material. U.S. Patent 8,460,631 B2.

Corathers, L.A. 2008. Manganese. In *Mineral Commodity Summaries*. Reston, VA: U.S. Geological Survey.

Corathers, L.A. 2014. Ferroalloys. *2012 Minerals Yearbook.* Reston, VA: U.S. Geological Survey.

Corathers, L.A. 2015. Manganese. In *Mineral Commodity Summaries*. Reston, VA: U.S. Geological Survey.

Cunningham, M. 2015. *Review of Manganese Prospects and Deposits in Indonesia.* Denver, CO: SRK Consulting.

Davis, J.R. 2001. High-strength low-alloy steels. In *Alloying: Understanding the Basics*. Materials Park, OH: ASM International. pp. 193–202.

Drzymala, J. 2007. *Mineral Processing: Foundations of Theory and Practice of Minerallurgy*, 1st English ed. Wroclaw: University of Technology.

Emsley, J. 2011. Manganese. In *Nature's Building Blocks: An A-Z Guide to the Elements.* New York: Oxford University Press. pp. 310–315.

Eramet. 2018. Comilog produced 4 million tons of manganese in 2017, Feb. 9. www.eramet.com/en/news/comilog-produced-4-million-tons-manganese-2017. Accessed July 2018.

Eramet Comilog. 2013. Silicomanganese. www.eramet.com/sites/default/files/eramet_silicomanganese_1.pdf. Accessed July 2018.

Eschler, P.Y., Lüthy, H., Reclaru, L., Blatter, A., Loeffel, O., Süsz, C., and Boesch, J. 2003. Copper-aluminium bronze—A substitute material for gold dental alloys? *Eur. Cells Mater.* 5:49–50.

Furlani, G., Pagnanelli, F., and Toro, L. 2006. Reductive acid leaching of manganese dioxide with glucose: Identification of oxidation derivatives of glucose. *Hydrometallurgy* 81:234–240.

Gajigo, O., Mutambatsere, E., and Adjei, E. 2011. *Manganese Industry Analysis: Implications for Project Finance.* Working Paper Series, no. 132. Tunis, Tunisia: African Development Bank.

Gilroy, A. 2014. Vale SA in the manganese and ferroalloys business. http://marketrealist.com/2014/12/vale-sa-manganese-ferroalloys-business/. Accessed December 2014.

Goonan, T.G., Jones, T.S., and Corathers, L.A. 2015. Manganese statistics. *In Historical Statistics for Mineral and Material Commodities in the United States*. USGS Data Series 140. Reston, VA: U.S. Geological Survey.

Gordon, Y., and Nell, J. 2013. Methods of manganese ore thermal-treatment prior to smelting—What to choose? In *The Thirteenth International Ferroalloys Congress: Efficient Technologies in Ferroalloy Industry*, Almaty, Kazakhstan. pp. 5–16.

Güler, E., Seyrankaya, A., and Cöcen, İ. 2008. Effect of Sulfation Roasting on Metal Extraction from Çinkur Zinc Leach Residue. *J. Ore Dress.* 10:1–10.

Gulf Manganese Corporation. 2015a. The elements of manganese. www.gulfmanganese.com/. Accessed August 2015.

Gulf Manganese Corporation. 2015b. *Timor Smelter Study*. South Perth, Western Australia: Gulf Manganese Corporation. http://gulfmanganese.com/wp-content/uploads/2016/07/25-May-2015-GMC-Timor-Smelter-Study-Combined.pdf. Accessed August 2015.

Gulson, B., Mizon, K., Taylor, A., Stauber, J.,Davis, J.M., Louie, H., Wu, M., and Swan, H. 2006. Changes in manganese and lead in the environment and young children associated with the introduction of methylcyclopentadienyl manganese tricarbonyl in gasoline—Preliminary results. *Environ. Res.* 100:100–114.

Gundewar, C.S. 2014a. *Manganese Ore: Vision 2020 and Beyond.* India: Indian Bureau of Mines.

Gundewar, C.S. 2014b. *Market Survey of Manganese Ore.* India: Indian Bureau of Mines.

Guo, X., Li, D., Park, K-H., Tian, Q., and Wu, Z. 2009. Leaching behavior of metals from a limonitic nickel laterite using a sulfation–roasting–leaching process. *Hydrometallurgy* 99:144–150.

Gustafsson, J.P. 2015. Minteq A2 database. http://vminteq.lwr.kth.se/download/. Accessed August 2015.

Gutzmer, J., and Beukes, N.J. 2009. Iron and manganese ore deposits: Mineralogy, geochemistry, and economic geology. In *GEOLOGY: Vol. IV, Encyclopedia of Life Support Systems*. Oxford: EOLSS. pp. 46–69.

Hein, J.R., and Koschinsky, A. 2013. Deep-ocean ferromanganese crusts and nodules. In *Treatise on Geochemistry*, 2nd ed. The Netherlands: Elsevier. pp. 273–291.

HHS (U.S. Department of Health and Human Services). 2012. *Toxicological Profile for Manganese*. Atlanta: HHS, Agency for Toxic Substances and Disease Registry.

Huang, H.-H. 2012. W32-STABCAL (software). Butte, MT: Montana Tech, Metallurgical Engineering.

Hudson Institute of Mineralogy. 2015. Mindat.org database [various minerals]. www.mindat.org/. Accessed December 2015.

IMA (International Magnetics Association). 2011. *Standard Recommendations: Soft Ferrite Cores, A User's Guide.* IMA-STD-100 2011.04. Cleveland, OH: IMA.

IMnI (International Manganese Institute). 2014. Applications—Industrial and metallurgical: Manganese and steelmaking. www.manganese.org/about-mn/applications/. Accessed August 2015.

IMnI (International Manganese Institute). 2016. *The Environmental Profile of Manganese Alloys*. Mississauga, ON: Hatch; Paris: IMnI.

Ismail, A.A., Ali, E.A., Ibrahim, I.A., and Ahmed, M.S. 2004. A comparative study on acid leaching of low grade manganese ore using some industrial wastes as reductants. *Can. J. Chem. Eng.* 82:1296–1300.

Kelly, T.D., and Matos, G.R., compilers. 2014. Manganese statistics. In *Historical Statistics for Mineral and Material Commodities in the United States*. USGS Data Series 140. Reston, VA: U.S. Geological Survey. https://minerals.usgs.gov/minerals/pubs/historical-statistics/ds140-manga.pdf. Accessed July 2018.

Key to Metals AG. 2010. Austenitic manganese steels. http://steel.keytometals.com/Articles/Art69.htm. Accessed August 2015.

Kilic, S., and Ozturk, F. 2014. Advanced high-strength steels in automotive industry to enhance sustainability. Presented at The 16th International Conference on Machine Design and Production, Izmir, Turkey, June.

Kosmulski, M., ed. 2009. *Surface Charging and Points of Zero Charge.* Boca Raton, FL: CRC Press.

Lasheen, T.A., El Hazek, M.N., and Helal, A.S. 2009. Kinetics of reductive leaching of manganese oxide ore with molasses in nitric acid solution. *Hydrometallurgy* 98:314–317.

Lawcock, G., Price, T., Battershill, J., Morgan, D., Brennan-Chong, J., and Bentvelzen, R. 2013. Manganese 101. UBS Investment Research, Australian Resources Weekly, October 23, 2013.

LeGrand, P. 2011. Electrochemical studies of passive film formation and corrosion of friction stir processed nickel aluminum bronze. M.S. thesis, Naval postgraduate school.

Matos, G.R., and Corathers, L.A. 2005. Manganese end-use statistics. Reston, VA: U.S. Geological Survey.

Mineral Resources Limited. n.d. Process Minerals International Pty Ltd. http://minrespublic.powercreations.com.au/entities/pmi.phtml. Accessed July 2018.

Nagpur Pyrolusite. n.d. Executive Summary. http://mpcb.gov.in/notices/pdf/ExeSum_NagpurPyrolusite.pdf. Accessed August 2015.

NRC (National Research Council). 2008. In *Minerals, Critical Minerals, and the U.S. Economy*. Washington, DC: National Academies Press. pp. 154–155.

Olivetti, E., Gregory, J., and Kirchain, R. 2011. *Life Cycle Impacts of Alkaline Batteries with a Focus on End-of-Life: A Study Conducted for the National Electrical Manufacturers Association.* Cambridge, MA: Massachusetts Institute of Technology, Materials Systems Lab.

Ostwald, J. 1975. Mineralogy of manganese oxides from Groote Eylandt. *Miner. Deposita* 10:1–12.

Papp, J.F., Corathers, L.A., Edelstein, D.L., Fenton, M.D., Kuck, P.H., and Magyar, M.J. 2007. Cr, Cu, Mn, Mo, Ni, and steel commodity price influences, Version 1.1. USGS Open-File Report 2007–1257. Reston, VA: U.S. Geological Survey.

Parc, S., Nahon, D., Tanov, Y., and Vieillard, P. 1989. Estimated solubility products and fields of stability for cryptomelane, nsutite, birnessite, and lithiophorite based on natural lateritic weathering sequences. *Am. Miner.* 74:466–475.

Pienaar, P.C., and Smith, W.F.P. 1992. A case study of the production of high-grade manganese sinter from low-grade Mamatwan manganese ore. In *INFACON 6: Proceedings of the 6th International Ferroalloys Congress*, Cape Town, Johannesburg, South Africa. pp. 131–138.

Pourbaix, M. 1974. *Atlas of Electrochemical Equilibria in Aqueous Solutions.* Houston, TX: NACE International. pp. 208, 488.

Rashad, M.M. 2006. Synthesis and magnetic properties of manganese ferrite from low grade manganese ore. *Mater. Sci. Eng. B* 127:23–129.

Rosenblum, S., and Brownfield, I.K. 2000. *Magnetic Susceptibilities of Minerals.* USGS Open-File Report 99-529. Reston, VA: U.S. Geological Survey.

South32. 2015. South Africa: Manganese. www.south32.net/our-operations/south-africa/manganese-south-africa. Accessed August 2015.

South32. 2017. What we do: GEMCO. https://www.south32.net/what-we-do/places-we-work/gemco. Accessed July 2018.

SPC (Secretariat of the Pacific Community). 2013a. *Deep Sea Minerals: Cobalt-rich Ferromanganese Crusts, A Physical, Biological, Environmental, and Technical Review.* Edited by E. Baker and Y.C. Beaudoin. New Caledonia: SPC.

SPC (Secretariat of the Pacific Community). 2013b. *Deep Sea Minerals: Manganese Nodules, A Physical, Biological, Environmental, and Technical Review.* Edited by E. Baker and Y.C. Beaudoin. New Caledonia: SPC.

Su, H., Wen, Y., Wang, F., and Tong, Z. 2009. Leaching of pyrolusite using molasses alcohol wastewater as a reductant. *Miner. Eng.* 22:207–209.

Su, H., Wen, Y., Wang, F., Sun, Y., and Tong, Z. 2008. Reductive leaching of manganese from low-grade manganese ore in H_2SO_4 using cane molasses as reductant. *Hydrometallurgy* 93:136–139.

Tan, W-F., Lu, S-J., Liu, F., Feng, X-H., He, J-Z., and Koopal, L.K. 2008. Determination of the point-of-zero charge of manganese oxides with different methods including an improved salt titration method. *Soil Sci.* 173:277–286.

Taneja, S.P., and Garg, V.K. 1993. Mossbauer and magnetic study of braunite mineral. *Nucl. Instrum. Methods Phys. Res.* B76:239–241.

Todd, M. 2010. Mn ore reduction technologies. Presented at the 7th IMnI EPD China Conference, Nanning, Guangxi, 23 March.

U.S. Mint. 2015. Coin and Medal Programs: Sacagawea golden dollar coin. Washington, DC: U.S. Mint. www.usmint.gov/mint_programs/golden_dollar_coin/?action=sacDesign. Accessed August 2015.

USGS (U.S. Geological Survey). 2016. Manganese. In Mineral Commodity Summaries. Reston, VA: USGS. https://minerals.usgs.gov/minerals/pubs/commodity/manganese/mcs-2016-manga.pdf.

Veglio, F., Trifoni, M., Pagnanelli, F., and Toro, L. 2001. Shrinking core model with variable activation energy: A kinetic model of manganiferrous ore leaching with sulphuric acid and lactose. *Hydrometallurgy* 60:167–179.

Wong, K. 2011. BHP Billiton to hike manganese capacity at Australia's Gemco JV. S&P Global Platts. https://www.spglobal.com/platts/en/market-insights/latest-news/metals/072911-bhp-billiton-to-hike-manganese-capacity-at-australias-gemco-jv. Northern Territory, Australia: Gemco. Accessed August 2015.

Woodward, R. 2001. Aluminum and aluminum alloys: Designations. www.azom.com/article.aspx?ArticleID=310#_Designations_for_Wrought. Accessed August 2015.

WorldAutoSteel. 2015. *FutureSteelVehicle Results and Reports & Cost Model*. Brussels, Belgium: WorldAutoSteel. www.worldautosteel.org/projects/future-steel-vehicle/phase-2-results/. Accessed August 2015.

You, Z., Li, G., Zhang, Y., Peng, Z., and Jiang, T. 2015. Extraction of manganese from iron rich MnO_2 ores via selective sulfation roasting with SO_2 Followed by water leaching. *Hydrometallurgy* 156:225–231.

Zhang, W., and Cheng, C.Y. 2007. Manganese metallurgy review. Part I: Leaching of ores/secondary materials and recovery of electrolytic/chemical manganese dioxide. *Hydrometallurgy* 89:137–159.

Zhang, W., Singh, P., and Muir, D. 2002. Oxidative precipitation of manganese with SO_2/O_2 and separation from cobalt and nickel. *Hydrometallurgy* 63:127–135.

Zhang, Y., You, Z., Li, G., and Jiang, T. 2013. Manganese extraction by sulfur-based reduction roasting–acid leaching from low-grade manganese oxide ores. *Hydrometallurgy* 133:126–132.

Zwicker, W.K., Groeneveld Meijer, W.O.J., and Jaffe, H.W. 1962. Nsutite—A widespread manganese oxide mineral. *Am. Mineral.* 47(99):246–266.